TOWARDS A 3D PRINTED MICROFLUIDIC PIN-FIN COOLER USING TWO PHOTON POLYMERIZATION (TPP)

Peter Sanchez, Ryan M. Price, and Robert C. Roberts
University of Texas at El Paso, USA

ABSTRACT

Thermal dissipation is a major problem faced by miniaturization of power systems. This has required new techniques to be developed for heat removal. Package-level microfluidic coolers are attractive as they offer a balance between thermal efficiency and ease of integration to conventional manufacturing processes. Two-Photon Polymerization (TPP) is a manufacturing technique which offers new opportunities for microscale structures and systems as it allows for the creation of three-dimensional structures that would be otherwise difficult to manufacture with conventional techniques. This work presents an opportunity to design microfluidic package coolers using TPP and perform evaluations on the resultant thermal resistances.

KEYWORDS

Two Photon Polymerization, Microfluidics, Packaging, Thermal Management, Pin Array

INTRODUCTION

Background

As silicon processes continue to shrink, the heat density and spot heating effects increase the demands on current cooling technologies. As clearly seen in a review for emerging wide and ultra-wide bandgap power devices, there is a clear pressure for new thermal management solutions that can be integrated at the package level [1]. Conventional packaged microelectronic devices for high power applications are often mounted with a heat spreading device that spreads generated waste heat from densified circuitry on die out over a larger surface in such way another technology or set of technologies, either passive or active, can then remove it. This introduces inefficiencies with several thermal interfaces being made between each of the thermal management system components [2].

The trend of combining multiple electronic and microsystems dies into a single package is driving a need for new solutions for 3D heterogeneous integration (3DHI). Electronic packages are quickly becoming a complex microsystem that can benefit from innovations to address the needs of future 3DHI systems. New strategies have focused cooling to be closer to the actual device as identified by [2], [3], [4]. One approach is die-level cooling. In this approach, cooling is integrated into the backside of the die itself [3]. This method is the most efficient method to cool a device as heat only needs to be transferred from the silicon to the cooling fluid on the other side of the die [3]. The disadvantage of this approach however is that it increases the complexity of device fabrication [4], [5]. An alternative approach to avoid this complexity is cooling at the package level [4], [5]. Package level cooling integrates cooling into the package from which a cooling fluid can be forced directly against the die [2]. This offers a more direct approach to escaping the inefficiency of thermal conduction between the package and an external cooler [2].

Two-Photon Polymerization

Two Photon polymerization (TPP) is an emerging manufacturing technique used for microfabrication. TPP uses a laser to selectively cure a photopolymer resin or photoresist, allowing direct writing of polymer microstructures [6]. This printed structure can be further processed or alternatively used as the device itself. [6] Unlike other techniques, which rely on single photon absorption, TPP can print much smaller structures as an effect of the two-photon absorption being a nonlinear optical process, so the intensity of the excitation can be focused on a small volume, instead of a column of material, as is the case for linear single-photon absorption [6]. For the system used in this work, a football shaped voxel can be realized with a diameter of ~160nm and a height of ~500nm, enabling true 3D microfabrication from photopolymer resins.

In previous work the fabrication method of Direct Metal Laser Sintering (DMLS) was studied. That technique resulted in a structure printed out of sintered 316L stainless steel [4], [5], [7]. The work presented in this paper builds on our fabrication process described in [4], [5], [7] which used DMLS metal 3D printing to fabricate various microfluidic package cooler designs and revealed that the fluid dominated in cooling performance. However, the 30μm layer thickness and 30μm laser diameter of the DMLS system limit the ability to fabricate complex 3D structures with microfabrication precision. From this, similar microfluidic cooler designs could be designed and fabricated using TPP to take advantage of its precision to create truly 3D microfabricated geometries to address the future needs of electronic packaging.

PACKAGE COOLERS

Package level cooling works closer to the die than system level cooling while not interfering with the manufacture of the die itself. Several distinct types of designs are common among microfluidic package coolers including open plenums, pin arrays and microfluidic channels which can be straight, wavy, or serpentine [5].

Previous work studied this assortment of designs applied to a 1cm die. In that work it was studied and determined that the pin array design offers the lowest thermal resistance when compared to channel designs [4]. For this reason, the pin array was selected as the basis for this study.

Rather than the standard cylindrical pins, new customized pins were created to have a helical twisted shape. These pins are similar to those studied in [8]. This work found that grooved pins resulted in the pin array having a greater heat transfer coefficient than a similar array of cylindrical pins [8]. This was true for pins with a square thread as well as a helical groove [8]. Similar performance benefits for grooved and threaded pin arrays were found in [9]. The superior thermal properties of grooved pins are due to their promotion of turbulent flow, causing greater mixing of the fluid in the cooler [8], [9]. For our pins, they took the shape of a 5-point star twisted by 180 degrees from the bottom to the top of the pin, which is 1500μm in its height. The star was designed to have a radius so that it is inscribed into a pentagon with a 250μm circumscribed radius. The CAD rendering and printed package are shown in Figure 1. The objective of this pin shape is to have helical channels for the fluid to flow through, with the intent to better allow thermal contact with the fluid and the underside of the packaged die.

The design used features a staggered array of grooved helical pins. Helical pins were used as they have been studied to promote turbulent flow [10]. In this work, it was experimentally shown that grooved pins resulted in a greater heat transfer coefficient from the fluid to the pin [10].

FABRICATION

Printing

As introduced, TPP allows for greater freedom in the designs used over the 2D lithography which is conventionally used at the micro scale. The helical pins which were used in [9] were macroscopic, 15mm in diameter and manufactured out of aluminum. TPP allows for similar pins to be made at a smaller scale, the chosen design had pins with a circumscribed radius of 250µm.

As discussed, prior, package coolers were fabricated using TPP. Specifically, the Nanoscribe Photonic Professional TPP printer was used. The Nanoscribe TPP printer offers various print modes using different objective lenses, substrates, and resins. Based on the previous works it was determined that the large features set which comes stock with the machine would be the most appropriate. This feature set uses the 10x objective, suited for the largest structures that the machine can print. However, even with the large feature set, it was determined that the Nanoscribe system was unsuited to printing packages at the same scale as the previous DMLS work; doing so would require excess printing time and serve poorly to demonstrate the micro-scale printing capabilities of the system. To adapt the package design to the Nanoscribe system, a 0.5cm^2 die size was used, as opposed to the original 1cm^2 size used for the DMLS work.

For printing with the 10x large feature set, IP-Q resin was used to print the packages on a silicon substrate. After a print was completed, it was cleaned of excess resin by being submerged in a bath of PGMEA for 20 minutes and then being placed in a bath of IPA for 5 minutes. This cleaning process is standard practice for all prints. The resulting printed pin array package is shown in Figure 1, where it is still attached to the silicon substrate on which it was printed. SEM imagery of the printed staggered pin array is shown in Figure 2. From Figure 2, the pins can be seen as they were designed and printed with their star-shaped faces and helical grooves. Figure 2 also shows the seams made in the printed structure as the Nanoscribe prints large structures of many divided blocks. By default, the system would print these blocks with 5µm overlaps, however, this setting was changed to print with a 20µm block overlap to ensure the structure would be well sealed so it could contain fluid.

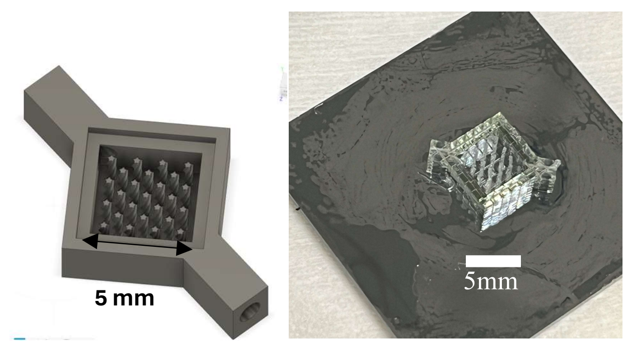

Figure 1: CAD model and device as printed in IP-Q Nanoscribe resin. This design features an array of 25 twisted pins in a staggered arrangement. Printed design accepts a 0.5cm^2 silicon die.

Package Construction

These printed packages were then removed from the printing substrates and made into packages. These package assemblies were then assembled by placing 20-gauge syringe needles in the inlet and outlet ports of the package. A piece of silicon wafer was cut to an area of 0.5cm^2 square and used as a silicon die for the package. The needles and die were then sealed to the printed package using CR Laurence UV692 Medium Viscosity UV resin. The fully assembled package with a die and needles is shown in Figure 3.

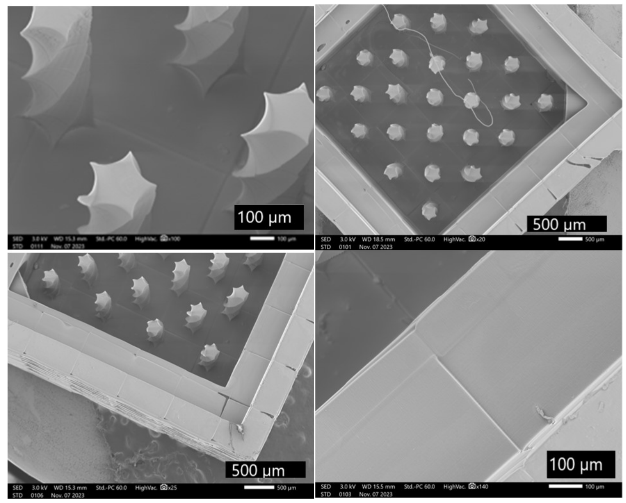

Figure 2: SEM images of printed device features. The seams observed in the images were due to galvanometer issues impacting the scan field of the 2PP system during manufacturing. A more ideal stitch can be observed in the lower right image. The length of white scale bars of each SEM are denoted by the black-boxed text.

Test Setup

For the test setup, there were several requirements it needed to fulfill. The test setup had to be able to pump fluid through the package, transfer heat to the die and allow for the temperature of the package die to be measured and recorded over time. To move fluid through the package, a 12V peristaltic pump was used. This pump moves cool water from one beaker, through the pump, into the package and then out to another beaker where the fluid was collected. To prevent heat from building up in the cooling fluid, the cooling water would only be circulated once. This open loop design is the same as our previous work [4], [5], [7] as well as the work presented in [2]. Heating of the die and temperature measurement were accomplished using a surface mount resistor and thermistor, respectively. The resistor and thermistor are mounted onto a piece of perfboard such that both are in good contact with the die surface. This was then clamped down to the die using two bolts and a 3D printed mount, shown in Figure 3. Temperature measurements were recorded from the thermistor by a microcontroller which were then transmitted over serial where they could be logged over time by a computer.

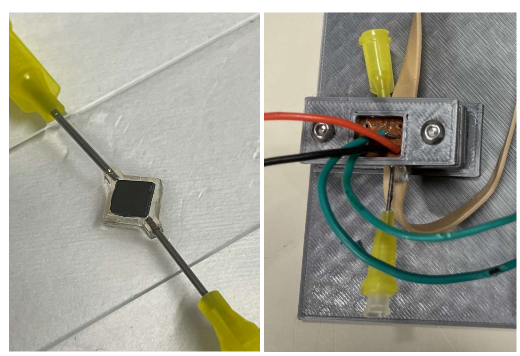

Figure 3: (Left) Sealed package with silicon die and fluidic ports. (Right) Test Sample with sample clamped in position for testing to a heater block with temperature sensors. A rubber band is placed on the backside of the package to prevent slipping against the 3D printed base.

TESTING

Two packages were made to be tested. First, a flow rate test was done to determine how much fluid could be pumped through the sample at 5 different voltage levels from 12V to 4V. Two thermal tests were designed with emphasis on measuring two main parameters, the die temperature, and the time elapsed. These parameters were then used to calculate the thermal resistance of the designed packages. To understand how the packages behave, a transient and steady state test were performed. The methodology of these tests follows that of [4], [7]. Both transient and steady-state tests were done on the two built packages. These tests were done on each package with and without fluid flow to examine its impact on cooling.

The transient thermal performance test was performed by heating the package until the temperature sensor reported a temperature of 50°C, at which point the power to the heater was removed. In tests involving fluid flow, the pump would also be turned on at this point. The pump was powered by a 12V DC source and consumed 2.4W of power to push fluid through either sample. The time for the package to cool back down was then recorded. The objective of this test is to reduce the time taken to cool back down.

The steady state test involved having a constant 0.5W heat load using resistive heating. A period of 1000 seconds would then be allowed to pass with the goal of giving the temperature time to stabilize. The temperature which the device would equilibrate at would then be recorded.

The results provided by the steady state test could also be used to calculate the thermal resistance of the package.

RESULTS

Flow Rate

Table 1 and Table 2 show the results of the flow rate test for each of the two samples, respectively. From these tables, the second of the two samples had a slightly higher flow rate than the first sample.

Table 1: Flow Rate Through Sample 1 At Various Pump Voltages

VOLTAGE (V)	POWER (W)	AVG FLOW RATE (ML/S)
12	2.40	1.02
10	2.00	0.94
8	1.44	0.77
6	0.96	0.57
4	0.60	0.34

Table 2: Flow Rate Through Sample 2 At Various Pump Voltages

VOLTAGE (V)	POWER (W)	AVG FLOW RATE (ML/S)
12	2.40	1.28
10	1.80	1.09
8	1.36	0.82
6	0.96	0.57
4	0.56	0.34

Transient Thermal Test

The results for the transient test are shown in Figure 4 and Table 3. This test shows that the packages cooled down faster when fluid flow was used. This was true for both packages which were constructed. Table 3 shows the cooling time for each of the packages with and without flow. Table 3 also shows the flow rate for each package at 12V as determined in the flow rate tests. Table 3 and Figure 4 both show that each package cooled faster with fluid flow. Note that in figure 4, the difference in heating time for the two packages was adjusted to align the peaks, as the purpose of this test is specifically to measure the cooling time. It can additionally be determined from Table 3 that sample 2 cooled 31.56 seconds faster than sample 1, without flow and sample 2 cooled 37.87 seconds faster than sample 1 with fluid flow. This difference could be partially explained by the fact that sample 2 had a flow rate 0.26mL/s faster than that of sample 1.

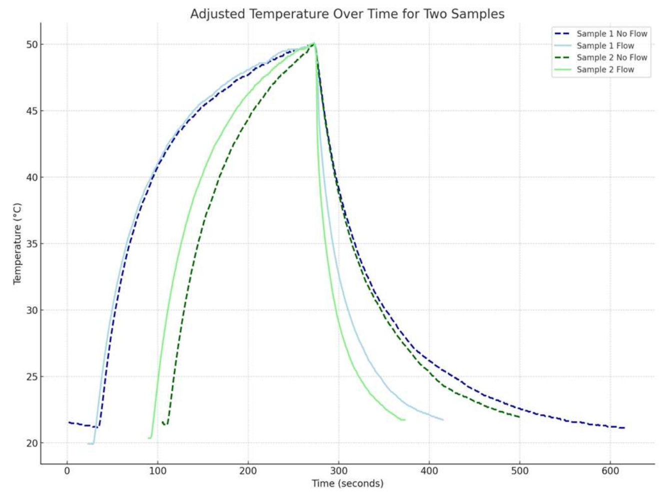

Figure 4. Transient thermal performance of two samples with and without fluid flow. Note that the tests for sample 2 appear to start heating later than the sample 1 test. This is the case because sample 2 heated faster, and its graphs were time shifted to align the peaks for all if the tests as the purpose was to measure the cooling time from 50°C to 22°C.

Table 3: Transient Cooling Time from 50°C to 22°C

Sample	Cooling Time (No Flow) (s)	Flow rate (mL/s)	Cooling time with (Flow) (s)
1	256.65	1.02	131.49
2	225.09	1.28	93.62

Steady-state Thermal Test

Figure 5 and Table 4 show the results for the steady state test. Again, it is seen that the package with fluid flow has better thermal performance than the one that does not. This thermal performance is characterized by the thermal resistance which was computed using the results from this test using the equation below following the method in [7]. ΔT represents the difference between the package temperature and the ambient temperature. *P* represents the power dissipated by the heater in steady-state operation.

$$R = \frac{\Delta T}{P} \quad (1)$$

Table 4: Steady state thermal resistance demonstrating a 37.5% improvement in fluidic cooling.

Condition	Temperature (Package) (°C)	Temperature (Ambient) (°C)	Thermal Resistance (°C/W)
No Flow	36.07	20.61	30.92
Flow	30.26	20.61	19.30

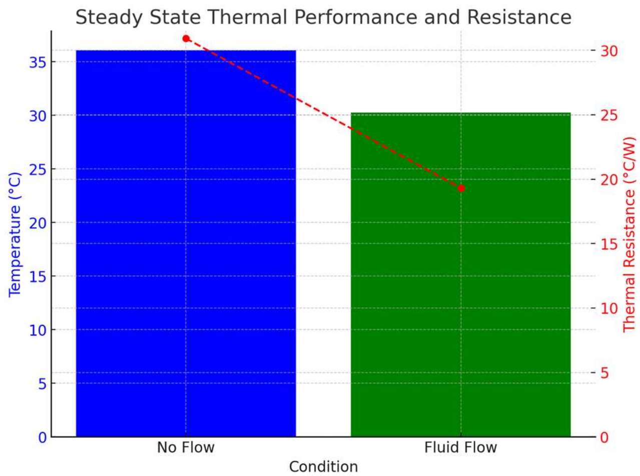

Figure 5: Steady-State thermal performance of package with and without fluid flow. The difference in thermal resistance is shown. With fluid flow, the temperature reached an equilibrium at 30.26°C, 5.81°C cooler than without flow.

FUTURE WORK

As this work builds on previous work using the DMLS printer, demonstrating a new design and fabrication technique, future work could focus on comparing packages of several designs, all made using TPP. These designs could consist of different shapes and orientations of pins, or new structures which further take advantage of TPP's unique ability to fabricate small 3D structures to increase fluid interaction with the microsystems die at the top of the channel. This future work could also include replicating previous work done using the DMLS printed design and translating them to TPP parts.

CONCLUSION

In conclusion it appears that a microfluidic pin array package cooler can be fabricated using TPP. The results of this preliminary work show that the packages can be cooled with fluid flow. Both tests indicate that the pin-array cooler can remove heat when fluid flow is present even though the cooler is made of a high thermal resistance resin material. Furthermore, the capabilities of TPP allow for the pins of the package cooler to have a complex 3D structure as opposed to only being simple pins.

ACKNOWLEDGEMENTS

This material is based upon work supported by the Department of Energy (National Nuclear Security Administration) under Award Number DE-NA0004110 and the Air Force Office of Scientific Research under award number FA9550-23-1-0477.

REFERENCES

[1]. Y. Qin, B. Albano, J Spencer, J.S. Lundh, B. Wang, C. Buttay, M. Tadjer, C. DiMarino, Y. Zhang, "Thermal management and packaging of wide and ultra-wide bandgap power devices: a review and perspective", *J. Phys. D: Appl. Phys*. 56, 093001 (2023).

[2]. J.Y. Chang, D. Kulkarni, R. Mahajan, M. Jorgensen, N. Neal, R. Dischler, A. Dasu, S. Ahuja, R. Mongia, "Package-Level Integration of Liquid Cooling Technology with Microchannel HIS for High Power Cooling," *20th IEEE Intersociety Conference on Thermal and Thermomechanical Phenomena in Electronic Systems (iTherm)*, 18-23 (2021).

[3]. S.K. Rajan, B. Ramakrishnan, H. Alissa, W. Kim, C. Belady, M.S. Bakir, "Integrated Silicon Microfluidic Cooling of a High-Power Overclocked CPU for efficient Thermal Management", *IEEE Access*, 10, 59259-59269 (2022).

[4]. B. Lohani, S. D. Hossain, and R. C. Roberts, "Metal Additive Microfabrication of System in Package with Embedded Microfluidic Thermal Management for Heterogeneous Integration with Semiconductor Dies", *Journal of Electronic Materials*, 52, 2940 (2023).

[5]. B. Lohani and R. C. Roberts, "Metal Additive Microfabricated Microfluidic Packages for Integrated Thermal Management In Power Application,", *21st International Conference on Micro and Nanotechnology for Power Generation and Energy Conversion Applications (PowerMEMS)*, 121 (2022).

[6]. J.T. Fourkas, *Three-Dimensional microfabrication using two-photon polymerization*, William Andrew Publishing, (2020).

[7]. B. Lohani, P. Sanchez and, R.C. Roberts, "Comparative Study of Different Microchannels for Microfluidic Packages with Integrated Thermal Management in Power Applications", *2023 IEEE 22nd International Conference on Micro and Nanotechnology for Power Generation and Energy Conversion Applications (PowerMEMS), 22, 214-217 (2023).*

[8]. J.A. Siddiqui, S. Lahane, A.V. Gadekar, and V. L. Lokawar, "Experimental and Computational Evaluation of Pressure Drop and Heat Transfer Characteristics in Rectangular Channel with Helix Grooved Profile Pin Fins", *Advances in Energy Research*, 1, 729 (2020).

[9]. M.R. Haque, T.J. Hridi and, M.M. Haque, "CFD studies on thermal performance augmentation of heat sink using perforated twisted, and grooved pin fins", International Journal of Thermal Sciences, 182, 107832 (2022).

[10]. S. Ashman, and S. G. Kandlikar, "A Review of Manufacturing Processes for Microchannel Heat Exchanger Fabrication", *Proceedings of the ASME 4th International Conference on Nanochannels, Microchannels, and Minichannels. ASME 4th International Conference on Nanochannels, Microchannels, and Minichannels, Parts A and B*, 855 (2006).

CONTACT

*P. Sanchez, tel: +1-915-588-4371; prsanchez4@miners.utep.edu